

## Band-gap energy of $\text{In}_x\text{Ga}_{1-x}\text{N}_y\text{As}_{1-y}$ as a function of N content

J.-Y. Duboz,\* J. A. Gupta, Z. R. Wasilewski, J. Ramsey, R. L. Williams, G. C. Aers, B. J. Riel, and G. I. Sproule  
*Institute for Microstructural Sciences, National Research Council, Ottawa, Ontario, Canada K1A 0R6*

(Received 14 March 2002; published 15 August 2002)

The band-gap energy of InGaNaNs decreases with N content at a smaller rate than that of GaNaNs. Precise absorption measurements in strained InGaNaNs/GaAs quantum wells on GaAs(001) are reported, and the result is explained in the frame of the repulsion between the nitrogen level and the  $\Gamma$  conduction band. As the energy separation between both levels is larger when the In content increases, the effect of introducing nitrogen is significantly reduced. In order to get a quantitative description of experimental results, the model includes a detailed description of the local N environment. Results suggest that in our InGaNaNs/GaAs quantum wells grown by molecular beam epitaxy, the N configuration should be close to the statistical one. Using this model to explain the effect of annealing on band structure, we conclude that, on average, N atoms gain one additional nearest-neighbor In atom during the annealing, leading to a moderately large band-gap blueshift of 20–30 meV.

DOI: 10.1103/PhysRevB.66.085313

PACS number(s): 73.21.Fg, 71.20.Nr, 78.67.De

Nitrogen-containing III-V alloys have in recent years emerged as a subject of considerable theoretical and experimental research interest, due to their very unique physical properties and a wide range of possible device applications (see Refs. 1 and 2 for an extensive review). Unlike conventional III-V semiconductor alloys where the band-gap energy of the alloy varies almost linearly between the band-gap energies of parental binary or ternary compounds (with a small quadratic correction or bowing parameter), N-containing alloys exhibit a very strongly nonlinear variation. For instance, substituting just 1% nitrogen for arsenic in GaAs decreases the band-gap energy from 1.42 to 1.25 eV at room temperature,<sup>3</sup> although the GaN band-gap energy is much higher (3.43 eV). Additional unusual observations were made, including the appearance of a higher energy level (so-called  $E_+$ ) that varies with N content,<sup>4–6</sup> a strongly increased electron mass,<sup>7,8</sup> a strong localization of electron wave functions,<sup>4</sup> and a strong reduction of the hydrostatic pressure coefficient of the band gap.<sup>4,6</sup> All these observations were explained by the coupling of a nitrogen level with the  $\Gamma$  conduction band.<sup>5,6,9,10</sup> The model was then improved by including the  $X$  and  $L$  coupling.<sup>11</sup> Alternatively, more sophisticated calculations were carried out to explain the physics of dilute nitrides and the exact nature of perturbed host states, cluster states, and the  $E_+$  state.<sup>12–14</sup> In InGaNaNs, an additional complication was recently noted. The exact value of the band-gap energy depends on local ordering and more precisely on N being bonded to In or Ga.<sup>15–19</sup> This latter property is likely to explain the observed blueshift of the band gap with annealing in InGaNaNs samples.<sup>16</sup>

In the present work, we have measured the dependence of the InGaNaNs band-gap energy with N concentration. We clearly show that this variation is much smaller in InGaNaNs than in GaNaNs. We also study the effect of annealing on the optical properties. We use our results and other data from the literature to show that the level repulsion model can give at least a good phenomenological description of the conduction band in InGaNaNs, provided ordering effects are taken into account.

The samples were grown by solid-source molecular beam epitaxy (MBE) in a modified VG V80H system. The In and

Ga fluxes were provided by thermal effusion cells, and As<sub>2</sub> was provided by a valved cracker cell. Active nitrogen was provided by an Applied Epi Unibulb radio frequency (rf) plasma source using Ar/N<sub>2</sub> dynamic gas switching.<sup>20</sup> The three samples discussed here were grown at approximately 455 °C and consist of five-period  $\text{In}_x\text{Ga}_{1-x}\text{N}_y\text{As}_{1-y}$ /GaAs multiple quantum wells (QW's) with nominal compositions of  $x=0.25$  and  $y=0, 0.005$  or  $0.010$ . Table I summarizes the thicknesses and compositions measured by high-resolution x-ray diffraction (HRXRD), with dynamical analysis using the BEDE Rads Mercury nonlinear least-squares package. In the following discussion, comparisons will be made between the properties of the samples before and after rapid thermal annealing (RTA), performed at 825 °C in flowing N<sub>2</sub> for 60 sec.

The photoluminescence (PL) was measured at room temperature, with a HeNe laser and a power density in the range of 50 W cm<sup>-2</sup>. Figure 1 shows the spectra. The PL peak shifts to lower energy as the N content increases, as expected. Annealed samples are blueshifted compared to as-deposited samples. The full width at half maximum (FWHM) increases with N content, from 32 meV in InGaAs to 38 and 45 meV for 0.5% and 1% nitrogen, respectively. After annealing, the FWHM is unchanged in InGaAs, while it is reduced to 34 and 40 meV for 0.5% and 1% nitrogen, respectively. Thus annealing reduces the nonuniformity by ordering the material. On the high-energy side of the spectra, a shoulder can be observed which will be interpreted later on. It could be argued that the PL does not measure intrinsic

TABLE I. Measured layer thicknesses and composition from HRXRD analysis. In the analysis the nitrogen composition was held fixed at the target value.

Sample	In composition, $x$	N composition, $y$	Thickness (Å)	Barrier Thickness (Å)
A	0.2349	0	66.5 ± 0.3	394 ± 2
B	0.2347	0.005	66.4 ± 0.3	393 ± 2
C	0.2298	0.010	65.5 ± 0.3	393 ± 2

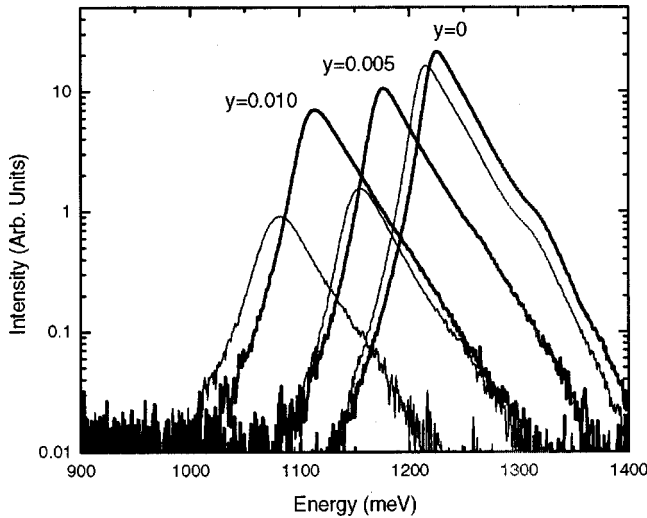


FIG. 1. Photoluminescence spectra at 300 K of  $\text{In}_x\text{Ga}_{1-x}\text{N}_y\text{As}_{1-y}/\text{GaAs}$  multiple quantum wells as-deposited (thin lines) and after RTA (thick lines). The incident power density is in the range of  $50 \text{ W cm}^{-2}$ .

transitions, but rather extrinsic transitions due to localization and band-gap tail states. Thus we measured the absorption of the backside-polished samples at room temperature. Transmission measurements were performed at normal incidence in a Bomen Fourier Transform InfraRed spectrometer. Figure 2 shows the transmission spectra of as-deposited samples. Three absorption steps can be observed, the first one having an amplitude of about 3%, while the second and third ones are about 2% large. The redshift with increasing N content is clear. Similar spectra were recorded in annealed samples. The width of the absorption steps (WAS) (defined from 10% to 90% of their maximum amplitude) can be evaluated from the spectra. The absolute width value cannot be compared directly with the FWHM of the PL spectra, but the relative variations can be compared. We found a very good correlation between both with  $\text{WAS} = 16 \text{ meV}$  in InGaAs: 29 and

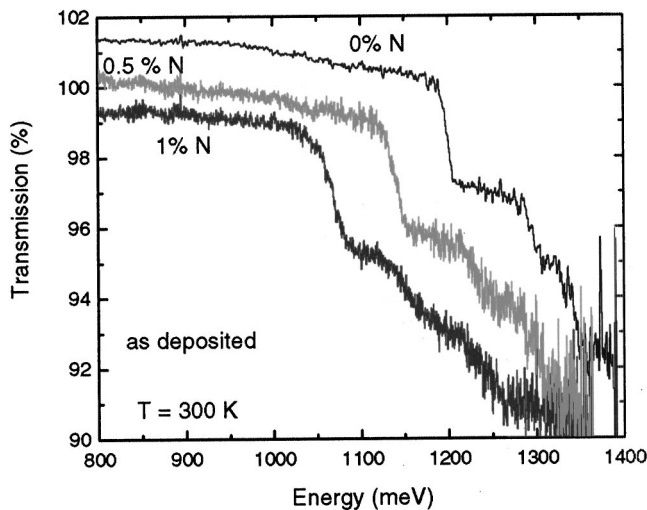


FIG. 2. Transmission spectra of as-deposited InGaAs/GaAs QW's. Curves are offset by 1% for clarity.  $T = 300 \text{ K}$ .

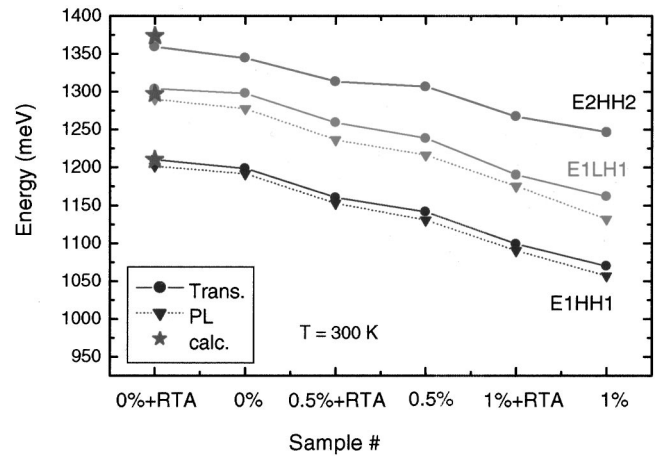


FIG. 3. Variation of transition energies measured by photoluminescence and absorption spectroscopy. Calculated  $e1-hh1$ ,  $e1-lh1$ , and  $e2-hh2$  are indicated for the InGaAs/GaAs QW.

32 meV in InGaAs with 0.5% and 1% N, respectively. Annealed InGaAs samples have a smaller WAS of 22 and 29 meV for 0.5% and 1% N, respectively.

Figure 3 summarizes all observations. The  $x$  axis is an arbitrary axis showing all six samples, with increasing N content and starting with the annealed samples. On the  $y$  axis, we report the PL peak and shoulder energies, and the absorption step energies. There is a perfect agreement between PL and absorption. Hence the PL spectra are dominated by intrinsic transitions, without any significant Stokes shift, and localization is not observed at room temperature. In the InGaAs/GaAs material system, we can rely on accurate calculations of energy levels in a quantum well. Figure 3 shows the results of these calculations which allow us to assign the three transitions to the  $e1-hh1$ ,  $e1-lh1$ , and  $e2-hh2$  transitions for increasing energies ( $hh$  and  $lh$  stand for heavy hole and light hole, respectively). We can thus confidently do the same assignment in the InGaAs quantum well. As a further confirmation, we also directly measured the intersubband transition  $e1-e2$  in all three samples in the far infrared. This is, to the best of our knowledge, the first intersubband observation in InGaAs and will be reported elsewhere.<sup>21</sup> We found the  $e1-e2$  energy in perfect agreement with our present near-infrared measurements. Many interesting features can be deduced from Fig. 3. First, the energy difference between  $e1-lh1$  and  $e1-hh1$  is constant for all samples. As the light-hole level in InGaAs is lower than the GaAs heavy-hole level, we actually have type-II transitions. Our data indicate that these transitions remain type II in InGaAs, showing that the valence band is not changed significantly when N is added in InGaAs, which was already reported by many authors.<sup>5,14</sup> We will assume that the valence-band structure is the same in InGaAs and InGaAs with the same In content. Second, we can fit the InGaAs band gap and effective masses from our data. We found that the electron mass increases from 0.056 in InGaAs to 0.089 and 0.095 in InGaAs with 0.5% and 1% N, respectively. It appears that InGaAs properties such as the optical transition widths (from PL or absorption) and the electron mass vary more when the N content increases from

0% to 0.5% than between 0.5% and 1%. This seems to indicate that the localized to delocalized transition, which was predicted by Kent and Zunger<sup>14</sup> to occur for about 0.6%, actually occurs for a smaller N content, as also suggested by Klar *et al.* for GaNAs.<sup>4</sup> This is also confirmed by the absence of a Stokes shift at 300 K in the sample with 0.5% N. The band-gap energy of as-deposited InGaNAAs samples was deduced to be 1142, 1074, and 1022 meV for 0%, 0.5%, and 1% N, respectively. We stress here that this type of study with a variation of one parameter only (N content) would have been very difficult to perform on bulk samples due to strain in InGaNAAs. Indeed, in thick InGaNAAs layers, both In and N compositions must be varied to keep the lattice matching with the GaAs substrate. In our pseudomorphically strained quantum wells, the band gap of InGaNAAs varies by 120 meV for 1% N substitution. We can now estimate the part of this variation due to strain. The InGaAs well is fully strained on GaAs. For a 53% In layer, the energy shift due to strain can be deduced from the comparison of InGaAs grown on GaAs and InP. The energy shift is 150 meV, with the  $hh$  level being the highest valence band in both cases. Assuming a linear variation for intermediate composition, the energy shift due to strain is about 3 meV for 1% In incorporated in a InGaAs well grown on GaAs. The comparison between atomic bonds shows that the lattice-matching condition in  $\text{In}_x\text{Ga}_{1-x}\text{N}_y\text{As}_{1-y}$  is kept when the In and N concentration variations are such that  $\Delta x \approx -3\Delta y$ . In other words, introducing 1% N is equivalent, from the strain point of view, to removing about 3% In. Hence this corresponds to a redshift of the band gap by about 10 meV for 1% N. We are now in a position to study the band-gap variation in strain-free InGaNAAs as a function of the N content. The band-gap reduction is 63 meV for 0.5% N and 110 meV for 1% N and strained free layers. This has to be compared with the 160-meV band-gap reduction for 1% N in GaNAs. It is of the same order of magnitude, but smaller. We would like now to quantitatively describe the band-gap variation of InGaNAAs with N content. To do so, we will make use of the two-level repulsion model.<sup>4,6,11,16</sup> We are aware that this model may not describe the intimate physics of the conduction band in InGaNAAs, especially for low-N content, and that more sophisticated calculations may be needed.<sup>14</sup> Supercell Monte Carlo calculations have predicted that the effect of N on the InGaNAAs band-gap energy should be smaller than the one in GaNAs.<sup>19</sup> For the time being, we simply use the repulsion model as a phenomenological approach. As we do not intend to describe the  $E_+$  band, we neglect here the  $X$  and  $L$  coupling.<sup>11</sup> The  $E_-$  level is given by

$$E_- = 0.5\{(E_N + E_C) - \sqrt{(E_N E_C)^2 + 4V^2 x}\}, \quad (1)$$

where  $E_C$  is the uncoupled conduction-band energy at the  $\Gamma$  point,  $E_N$  is the energy of the N level, and  $V$  is the off-diagonal term of the Hamiltonian describing the coupling between the N level and  $\Gamma$  conduction band. Full  $sp^3s^*$  tight-binding supercell calculations suggest that  $V$  varies from  $V_{\text{Ga}} = 2$  eV to  $V_{\text{In}} = 1.35$  eV when the four N nearest neighbors (NN) are Ga or In, respectively,<sup>16</sup> which are the so-called four Ga NN and four In NN configurations.

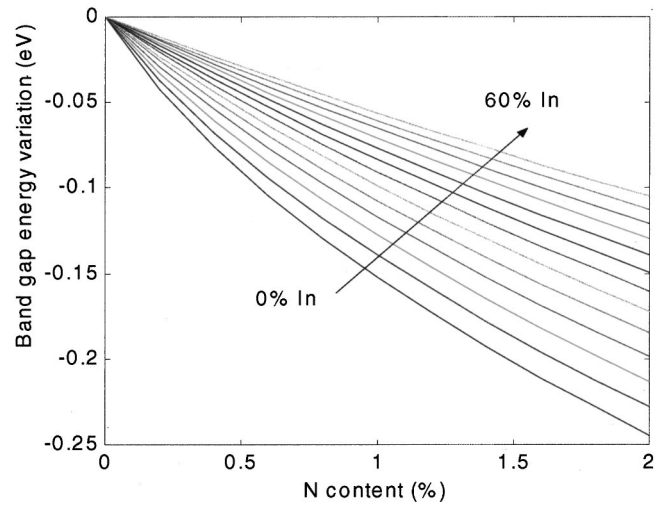


FIG. 4. Calculated band-gap energy variation with N content, with InGaAs as a reference. The In content varies from 0% to 60% by steps of 5%. We used the two-level repulsion model, where a statistical N environment is taken into account.

Experiments,<sup>4,11</sup> however, indicate that  $V_{\text{Ga}} = 2.4$  eV is better suited in GaNAs, i.e., in the four Ga NN configuration. We do not have any experimental data for InAsN, but we consistently modify  $V_{\text{In}}$  so as to keep a constant energy difference  $V_{\text{Ga}} - V_{\text{In}}$ , so that we take  $V_{\text{In}} = 1.75$  eV. It was also suggested<sup>16</sup> that the N-level energy depends on N configuration and In content:

$$E_N = E_{\text{Ga}} + i(E_{\text{In}} - E_{\text{Ga}})/4 - y\beta, \quad (2)$$

where  $E_{\text{Ga}} = 1.65$  eV,  $E_{\text{In}} = 1.9$  eV,  $\beta = 0.56$  eV, and  $i$  ( $i = 0-4$ ) describes the number of In neighbors in the N environment. Note that the N-level energy decreases with a slope of 5.6 meV for 1% In, while the InGaAs band gap reduces with a slope of about 10 meV for 1% In. Thus the energy separation between the N level and the InGaAs  $\Gamma$  conduction band increases with increasing In composition. The question now is to decide on the N environment in InGaNAAs. If samples are grown at moderate temperature (the usual case of molecular beam epitaxy), we can make the assumption that the local N environment is statistical or  $i = 4y$  and  $V = V_{\text{Ga}}(1-y) + V_{\text{In}}y$ . As the growth temperature is raised, the In NN configuration is favored as the local strain due to the small size of N atoms is relieved and as atomic motion on free surfaces is easy. After growth, when samples are annealed, the atomic motion is more limited, and we will make the assumption that, on average, one additional In atom comes in the close vicinity of N atoms. This means that  $y$  is replaced by  $y + 0.25$  in the  $V$  expression, and  $i$  is replaced by  $i + 1$  in the  $E_N$  expression.

Figure 4 shows the band-gap reduction for strain-free InGaNAAs as a function of N and for various In concentrations. The GaNAs variation is of course well reproduced. We observe that the energy variation for 23% In is about 56 meV for 0.5% N and 100 meV for 1% N, which is very close to the experimental value. The literature confirms that InGaNAAs layers with a low In content ( $<10\%$ ) exhibit a large band-

TABLE II. Experimental and calculated energy shift in InGaNaNs, with InGaAs as a reference. The measured values are taken from the literature, with some elementary treatment to extract the band gap. The effect of strain is not taken into account here.

Reference	6	10	5	23	23	23	24	22	22
% In, % N	8, 2.3	4, 1	5, 1.3	34, 0.7	38, 5.2	41, 3.1	23, 5	56, 1	59, 3.2
Experiment (meV)	250	160	190	50	298	201	376	43	<107
Calculated (meV)	240	141	168	59	294	191	350	46	155

gap shift, while layers with a high In content show a smaller band-gap reduction. Table II summarizes the comparison between experimental values from the literature and the calculated ones. The following calculations were made, when necessary, in order to extract the band gap from the published data. When not measured, the band gap in InGaNaNs with the same In content as the InGaNaNs was calculated using standard extrapolation formulas. In quantum wells, the electron and hole confinement energies are calculated and subtracted from the transition energy to give the band-gap energy. This procedure may introduce some error, which we estimate to be of the order of 10–20 meV depending on the cases. Table II shows the good agreement between calculated and measured values. It is interesting to note that even films grown on InP with a very high In content<sup>22</sup> seem to follow the same law. Discrepancies can be explained by experimental uncertainty in the actual composition, errors in our extraction of the band gap, or some special N configuration that does not follow the statistical distribution.

We would like now to address the effect of annealing. Annealed samples are blueshifted by 22 and 29 meV for 0.5% and 1% N, respectively. We also measured the  $e1-hh1$  transition in InGaNaNs/GaAs quantum wells, with 30% In and 2% N. The absorption edge shifted after annealing by about 20 meV. The calculation, assuming that one additional In atom comes in the vicinity of N atoms, gives an energy difference of 26 meV, which agrees well with our observations. The one In atom movement is in agreement with far-infrared measurements of Ga-N and In-N stretches<sup>15</sup> and electromodulated and photomodulated reflectance studies of InGaNaNs laser structures.<sup>17</sup> Larger band-gap energy shifts after annealing have also been observed,<sup>16</sup> increasing from 0 to about 30 meV when the In content increases from 0% to 10%, then remaining equal to 30 meV, and increasing again

to about 60 meV for In content larger than 25%. These two steps are explained in terms of one, then two In atoms moving during the annealing. When the growth conditions are such that the initial configuration is four Ga NN, then the annealing is more likely to move a larger number of In atoms and the blueshift is larger.<sup>16</sup> In our case, it is likely that the initial configuration was statistical and thus close to three GaIn NN, so that only one atom motion was observed during annealing. Recent theoretical studies explained this tendency for In atoms to move closer to N atoms.<sup>19</sup> The strain energy, which tends to bond In to N and Ga to As, is larger than the cohesive energy that would favor the formation of GaN and InAs.

Finally, let us note that the situation in thin quantum wells and in bulk material may be quite different with regards to the local ordering and reordering during annealing. Phenomena such as In segregation, surface reconstruction, or strain during the growth are different in both cases. Dynamic effects are likely to play a larger role in heterostructures than in bulk and may in the case of thin quantum wells surpass thermodynamic effects. Molecular beam epitaxy should be a powerful tool to precisely study these dynamic effects, and significant progress in this field is to be expected in the near future.

In conclusion, the InGaNaNs band-gap energy variation with N content is smaller than the one in GaNaNs. This is due to the N level being farther away from the  $\Gamma$  conduction band in InGaNaNs and to the level coupling being smaller. The two-level repulsion model can be used, at least for N contents larger than 0.5%, with the condition that the N environment be carefully taken into account. This model also permits an explanation of the effect of annealing on the band-gap energy.<sup>23,24</sup>

\*Also at Thales Research and Technology, 91404 Orsay, France. Electronic address: jean-yves.duboz@nrc.ca

<sup>1</sup>I. A. Buyanova, W. M. Chen, and B. Monemar, *MRS Internet J. Nitride Semicond. Res.* **6**, 2 (2001).

<sup>2</sup>*Low-Dimensional Nitride Semiconductors*, edited by Bernard Gil (Oxford University Press, Oxford, 2002).

<sup>3</sup>M. Weyers, M. Sato, and H. Ando, *Jpn. J. Appl. Phys., Part 2* **31**, L853 (1992).

<sup>4</sup>P. J. Klar, H. Gruning, W. Heimrodt, J. Koch, F. Hohnsdorf, W. Stolz, P. M. A. Vicente, and J. Camassel, *Appl. Phys. Lett.* **76**, 3439 (2000).

<sup>5</sup>J. D. Perkins, A. Mascarenhas, Yong Zhang, J. F. Geisz, D. J. Friedman, J. M. Olson, and Sarah R. Kurtz, *Phys. Rev. Lett.* **82**, 3312 (1999).

<sup>6</sup>W. Shan, W. Walukiewicz, J. W. Ager III, E. E. Haller, J. F. Geisz, D. J. Friedman, J. M. Olson, and S. R. Kurtz, *Phys. Rev. Lett.* **82**, 1221 (1999).

<sup>7</sup>P. N. Hai, W. M. Chen, I. A. Buyanova, H. P. Xin, and C. W. Tu, *Appl. Phys. Lett.* **77**, 1843 (2000).

<sup>8</sup>M. Hetterich, M. D. Dawson, A. Yu. Egorov, D. Bernklau, and H. Riechert, *Appl. Phys. Lett.* **76**, 1030 (2000).

<sup>9</sup>A. Lindsay and E. P. O'Reilly, *Solid State Commun.* **112**, 443 (1999).

<sup>10</sup>P. Perlin, P. Wisniewski, C. Skierbiszewski, T. Suski, E. Kaminska, S. Subramanya, E. Weber, D. E. Mars, and W. Walukiewicz, *Appl. Phys. Lett.* **76**, 1279 (2000).

<sup>11</sup>B. Gil, *Solid State Commun.* **114**, 623 (2000).

<sup>12</sup>E. D. Jones, N. A. Modine, A. A. Allerman, S. R. Kurtz, A. F.

- Wright, S. T. Tozer, and X. Wei, Phys. Rev. B **60**, 4430 (1999).
- <sup>13</sup>T. Mattila, S. H. Wei, and A. Zunger, Phys. Rev. B **60**, R11 245 (1999).
- <sup>14</sup>P. R. C. Kent and A. Zunger, Phys. Rev. Lett. **86**, 2613 (2001).
- <sup>15</sup>Sarah Kurtz, J. Webb, L. Gedvilas, D. Friedman, J. Geisz, J. Olson, R. King, D. Joslin, and N. Karam, Appl. Phys. Lett. **78**, 748 (2001).
- <sup>16</sup>P. J. Klar, H. Gruning, J. Koch, S. Schafer, K. Volz, W. Stolz, W. Heimrodt, A. M. Kamal Saadi, A. Lindsay, and E. P. O'Reilly, Phys. Rev. B **64**, 121203(R) (2001).
- <sup>17</sup>S. A. Choulis, T. J. C. Hosea, P. J. Klar, M. Hofmann, and W. Stolz, Appl. Phys. Lett. **79**, 4277 (2001).
- <sup>18</sup>Steven Kurtz, J. F. Klem, A. A. Allerman, R. M. Sieg, C. H. Seager, and E. D. Jones, Appl. Phys. Lett. **80**, 1379 (2002).
- <sup>19</sup>K. Kim and A. Zunger, Phys. Rev. Lett. **86**, 2609 (2001).
- <sup>20</sup>J. A. Gupta, Z. R. Wasilewski, B. J. Riel, J. Ramsey, G. C. Aers, R. L. Williams, G. I. Sproule, A. Perovic, D. D. Perovic, T. Garanzotis, and A. J. Springthorpe (unpublished).
- <sup>21</sup>J. Y. Duboz *et al.* (unpublished).
- <sup>22</sup>M. R. Gokhale, J. Wei, H. Wang, and S. R. Forrest, Appl. Phys. Lett. **74**, 1287 (1999).
- <sup>23</sup>M. Bissiri, V. Gaspari, A. Polimeni, G. Baldassari Hoger von Hogersthal, M. Capizzi, A. Frova, M. Fischer, M. Reinhardt, and A. Forchel, Appl. Phys. Lett. **79**, 2585 (2001).
- <sup>24</sup>E. Tournie, M. A. Pinault, S. Vezian, J. Massies, and O. Tottereau, Appl. Phys. Lett. **77**, 2189 (2000).